

A Representation of Acoustic Waves in Unbounded Domains

BRADLEY K. ALPERT

National Institute of Standards and Technology

AND

YU CHEN

Courant Institute

Abstract

Compact, time-harmonic, acoustic sources produce waves that decay too slowly to be square-integrable on a line away from the sources. We introduce an inner product, arising directly from Green's second theorem, to form a Hilbert space of these waves and present examples of its computation.¹ © 2005 Wiley Periodicals, Inc.

1 Introduction

Consider the scattering problem governed by the Helmholtz equation

$$(1.1) \quad \Delta\varphi + k^2(1 + q)\varphi = 0$$

in two dimensions for a scatterer $q \in L^2(D)$ supported in a compact domain D in the half-plane above the x -axis. A function $u : \mathbb{R}^2 \rightarrow \mathbb{C}$ is referred to as a scattered wave, or an outgoing wave, from D if it has the form

$$(1.2) \quad u(\mathbf{r}) = \int_D H_0(k|\mathbf{r} - \mathbf{r}'|)\eta(\mathbf{r}')d\mathbf{r}'$$

for some $\eta \in L^2(D)$. As is well known, u satisfies the radiation condition

$$(1.3) \quad \frac{\partial u}{\partial r} - iku = o(r^{-1/2}), \quad r = |\mathbf{r}|,$$

and when restricted to a line such as the x -axis (see Figure 2.1), u decays at the rate of $O(r^{-1/2})$. Therefore u is not an L^2 function, and we cannot apply the standard inner product

$$(1.4) \quad (f, g) = \int_{-\infty}^{\infty} f(x)\bar{g}(x)dx.$$

¹Contribution of U.S. government not subject to copyright in the United States.

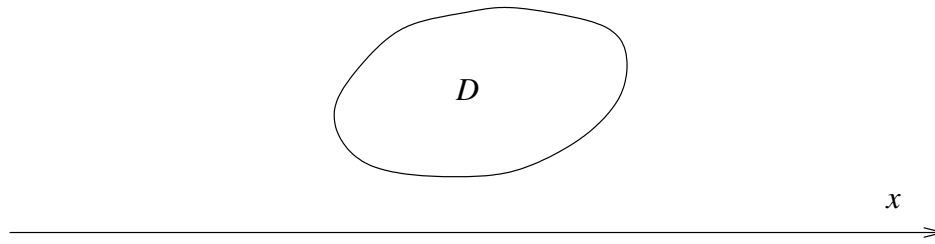


FIGURE 2.1. The scatterer D above the x -axis.

There are several applications for which an outgoing wave may need to be sampled and processed on a line. First, for wave scattering or propagation problems in a stratified host medium or in a wave guide, we may have to process wave functions on a line in two dimensions or a plane in three dimensions. Second, for a scatterer in a homogeneous host medium, it may be more convenient, efficient, and stable to process its scattered waves on a line as opposed to a closed curve containing D .

The lack of compact support of such functions makes their sampling and processing seem difficult. We introduce in this paper an inner product and use it to construct an orthogonal basis for all outgoing waves from D . In other words, we will present a method to efficiently sample the outgoing wave functions on the line.

2 The Inner Product

For simplicity, we will assume that the domain D is a positive distance from, as well as above, the x -axis; see Figure 2.1 and Remark 2.4. Denote by \mathcal{W} the linear space of functions that are restrictions to the x -axis of the outgoing waves $u(x, y)$ from D . In other words, let $A : L^2(D) \rightarrow C^\infty(\mathbb{R})$ be defined by

$$(2.1) \quad u(x) = (A\eta)(x) := \int_D H_0(k\rho) \eta(x', y') dx' dy'$$

with

$$\rho = [(x - x')^2 + y'^2]^{1/2}.$$

Then \mathcal{W} is the range space of A . With the negative y -direction as the outward normal, we will denote by $u_n(x)$ the normal derivative of u on the x -axis:

$$\begin{aligned} u_n(x) &= - \int_D \frac{\partial H_0(k\sqrt{(x - x')^2 + (y - y')^2})}{\partial y} \Big|_{y=0} \eta(x', y') dx' dy' \\ &= - \int_D k H_1(k\rho) \frac{y'}{\rho} \eta(x', y') dx' dy'. \end{aligned}$$

Therefore, for any $u \in \mathcal{W}$,

$$(2.2) \quad u(x) = O(|x|^{-1/2}), \quad u_n(x) = O(|x|^{-3/2}).$$

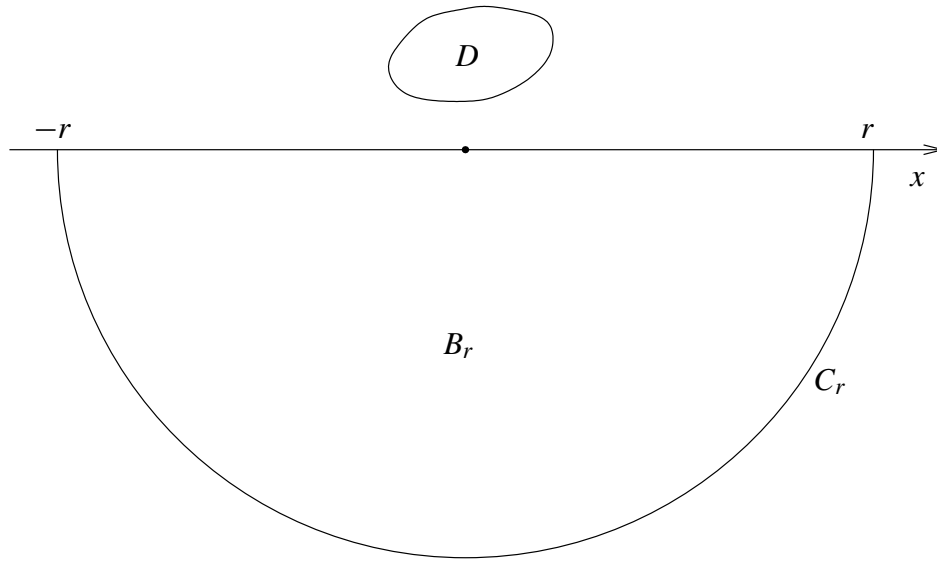


FIGURE 2.2. The scatterer D , semicircle C_r , and half-disk B_r .

THEOREM 2.1 For $u, v \in \mathcal{W}$, the bilinear form

$$(2.3) \quad (u, v) = \frac{i}{4} \int_{\mathbb{R}} [u(x) \bar{v}_n(x) - \bar{v}(x) u_n(x)] dx$$

is bounded and defines an inner product for \mathcal{W} .

PROOF: The existence of the integral for (u, v) follows immediately from (2.2). The bilinearity and symmetry of (u, v) are straightforward to verify. Now, we establish the positivity $(u, u) > 0$ for a nonvanishing $u \in \mathcal{W}$. In the lower half-plane, consider the semicircle

$$(2.4) \quad C_r = \{(x, y) : x^2 + y^2 = r^2, y \leq 0\}$$

and the half-disk B_r bounded by C_r and the interval $[-r, r]$ on the x -axis; see Figure 2.2. Let $v = \bar{u}$ in Green's second theorem

$$(2.5) \quad \int_{B_r} [u \cdot (\Delta + k^2)v - v \cdot (\Delta + k^2)u] dx dy = \int_{\partial B_r} \left(u \frac{\partial v}{\partial n} - v \frac{\partial u}{\partial n} \right) ds,$$

where $u(x, y)$ on B_r is the continuation of $u(x)$ on the line to the lower half-plane; see (1.2) and (2.1). It follows from $(\Delta + k^2)\bar{u} = 0$ in B_r that

$$(2.6) \quad \int_{-r}^r [u \bar{u}_n - \bar{u} u_n] dx = \int_{C_r} \left[u \frac{\partial \bar{u}}{\partial n} - \bar{u} \frac{\partial u}{\partial n} \right] ds.$$

The last integral we denote by $I(r)$. Integrating the radiation condition (1.3) over C_r yields

$$(2.7) \quad \int_{C_r} \left| \frac{\partial u}{\partial n} - iku \right|^2 ds = \int_{C_r} \left[\left| \frac{\partial u}{\partial n} \right|^2 + k^2 |u|^2 \right] ds - ikI(r) \rightarrow 0, \quad r \rightarrow \infty.$$

It follows from (2.3), (2.6), and (2.7) that

$$(2.8) \quad (u, u) = \frac{1}{4k} \lim_{r \rightarrow \infty} \int_{C_r} \left[\left| \frac{\partial u}{\partial n} \right|^2 + k^2 |u|^2 \right] ds.$$

Therefore, $(u, u) = 0$ implies that the 2-norm over $[\pi, 2\pi]$ of the far field $u_\infty(\theta)$ is 0. It follows from the analyticity of u_∞ that u_∞ is 0; therefore, u vanishes outside D ; in particular, $u \in \mathcal{W}$ is 0. \square

Remark 2.2. For the time-harmonic outgoing wave u , (u, u) is a constant multiple of its energy flux over a period and through the x -axis. The naturally induced norm $\|u\| = (u, u)^{1/2}$ makes \mathcal{W} a pre-Hilbert space.

The next lemma is a direct consequence of the boundedness of the linear map A and completeness of its domain $L^2(D)$.

LEMMA 2.3 *The linear space \mathcal{W} is complete, and therefore is a Hilbert space, with the inner product (2.3).*

Remark 2.4. It follows from the boundedness of the kernel $H_0(k\rho)$ of the integral operator A defined in (2.1) that the bounded linear map A is compact and has a singular value decomposition (SVD). It is not difficult to show that A is compact when D and the x -axis are not separated.

Remark 2.5. An orthogonal basis for \mathcal{W} can be computed via the SVD of A . In practice, the SVD will not be performed on A for fear of inefficiency, but on a map related to standard-layer potentials, such as the combined-layer potential (see, e.g., [2, p. 47]), whose domain is a set of functions defined on the boundary ∂D .

3 The Inner Product for Two Point Sources

In this section, we calculate the inner product for wave functions, each generated by a point source in D . On one hand, this calculation will be useful for computing the SVD of A or its equivalent layer potential representation (see Remark 2.5); on the other hand, it will demonstrate how an outgoing wave function from D should be finitely sampled on \mathbb{R} .

3.1 Inner Product for Two Monopoles

We refer to the function $u(\mathbf{r}) = H_0(k|\mathbf{r} - \mathbf{r}'|)$ as the wave generated by a monopole at $\mathbf{r}' \in \mathbb{R}^2$.

THEOREM 3.1 *Suppose that u and v are generated by two monopoles at $\mathbf{b}, \mathbf{c} \in D$. Then the inner product (u, v) depends only on the vector*

$$(3.1) \quad \mathbf{a} = \mathbf{b} - \mathbf{c} = (x_a, y_a).$$

More precisely, let $a = |\mathbf{a}|$ and let $\phi = \arctan(y_a/x_a)$ be the angle formed by the x -axis and \mathbf{a} . Then

$$(3.2) \quad (u, v) = \frac{1}{\pi} \int_{-\pi/2}^{\pi/2} e^{-ika \sin(\theta-\phi)} d\theta.$$

Thus $\operatorname{Re}(u, v) = J_0(ka)$ is independent of ϕ . Furthermore, when $\mathbf{b} = \mathbf{c} \in D$,

$$(3.3) \quad (u, u) = 1.$$

PROOF: As shown in Figure 3.1, we replace the integral over $[-r, r]$ with one along the semicircle,

$$(3.4) \quad \begin{aligned} (u, v) &= \lim_{r \rightarrow \infty} \frac{i}{4} \int_{-r}^r [u\bar{v}_n - \bar{v}u_n] dx \\ &= \lim_{r \rightarrow \infty} \frac{i}{4} \int_{\pi}^{2\pi} \left[u(r, \theta) \frac{\partial \bar{v}(r, \theta)}{\partial r} - \bar{v}(r, \theta) \frac{\partial u(r, \theta)}{\partial r} \right] r d\theta, \end{aligned}$$

where the integrand of (3.4) is simplified by the far-field asymptotics of wave functions u and v due to the two monopoles. The following two steps furnish the details of the proof.

(i) **GEOMETRY OF THE TWO SOURCES.** We suppose that in polar coordinates $\mathbf{r} = (r, \theta)$ with $\theta \in [\pi, 2\pi]$ and $\mathbf{b} = (b, \beta)$, $\mathbf{c} = (c, \gamma)$, with $\beta, \gamma \in (0, \pi)$; see Figure 3.1. The cosine law gives the distances $\rho = |\mathbf{r} - \mathbf{b}|$ and $\sigma = |\mathbf{r} - \mathbf{c}|$:

$$(3.5) \quad \rho^2 = b^2 + r^2 - 2br \cos(\theta - \beta),$$

$$(3.6) \quad \sigma^2 = c^2 + r^2 - 2cr \cos(\theta - \gamma).$$

From the pair of vertical sides and pair of horizontal sides of the dashed-line rectangle in Figure 3.1, we observe

$$\begin{aligned} -a \sin \phi &= c \sin \gamma - b \sin \beta, \\ -a \cos \phi &= c \cos \gamma - b \cos \beta. \end{aligned}$$

We multiply the first equation by $-\cos \theta$, multiply the second by $\sin \theta$, and add to obtain

$$(3.7) \quad -a \sin(\theta - \phi) = c \sin(\theta - \gamma) - b \sin(\theta - \beta).$$

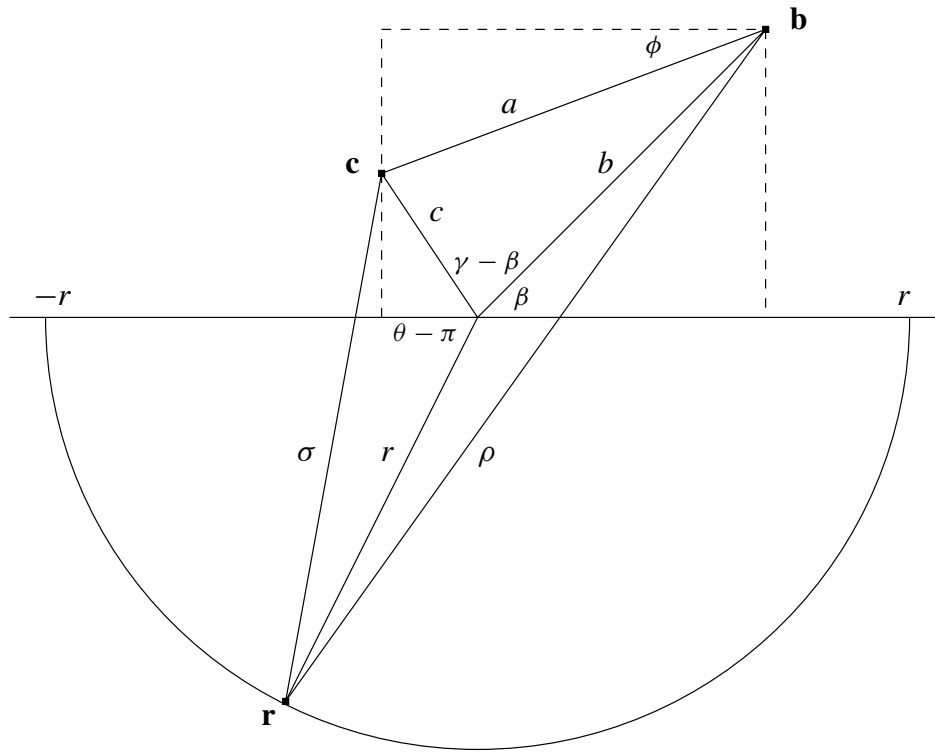


FIGURE 3.1. The source points **b** and **c** and field point **r** in polar coordinates.

(ii) FAR-FIELD ASYMPTOTICS. The monopoles are given by

$$(3.8) \quad u(\mathbf{r}) = H_0(k\rho), \quad v(\mathbf{r}) = H_0(k\sigma),$$

with their normal derivatives given by

$$(3.9) \quad \frac{\partial u(\mathbf{r})}{\partial r} = -kH_1(k\rho) \frac{\partial \rho}{\partial r}, \quad \frac{\partial v(\mathbf{r})}{\partial r} = -kH_1(k\sigma) \frac{\partial \sigma}{\partial r}.$$

The derivatives $\partial\rho/\partial r$ and $\partial\sigma/\partial r$ both approach 1 as $r \rightarrow \infty$; since both terms of the integrand are bounded, these derivatives can be ignored. The large-argument asymptotic expansion for the Hankel functions (see, e.g., [1, 9.2.3])

$$(3.10) \quad H_\nu(r) \sim \sqrt{\frac{2}{\pi r}} e^{i(r - \nu\pi/2 - \pi/4)} + O(r^{-3/2})$$

and the asymptotic expansion of ρ and σ from (3.5) and (3.6),

$$(3.11) \quad \rho \sim r - b \cos(\theta - \beta) + O(r^{-1}), \quad \sigma \sim r - c \cos(\theta - \gamma) + O(r^{-1}),$$

as $r \rightarrow \infty$, combined with (3.4), (3.8), and (3.9), yield

$$(3.12) \quad (u, v) = \frac{1}{\pi} \int_{\pi}^{2\pi} e^{ik(c \cos(\theta - \gamma) - b \cos(\theta - \beta))} d\theta.$$

We shift the integration to $[-\frac{\pi}{2}, \frac{\pi}{2}]$ and employ (3.7) to obtain (3.2). □

3.2 Inner Product for a Monopole and a Dipole

Suppose that $u_{\mathbf{r}'}(\mathbf{r})$ is the wave function generated by a monopole at $\mathbf{r}' \in \mathbb{R}^2$, and $\mathbf{d} \in \mathbb{R}^2$ is a unit vector, with polar coordinates $(1, \nu)$. Then the wave function generated by a dipole at \mathbf{r}' in orientation ν is defined as

$$\begin{aligned} v(\mathbf{r}) &= \lim_{t \rightarrow 0} \frac{u_{\mathbf{r}'}(\mathbf{r} + t\mathbf{d}) - u_{\mathbf{r}'}(\mathbf{r})}{t} \\ (3.13) \quad &= -\lim_{t \rightarrow 0} \frac{u_{\mathbf{r}'+t\mathbf{d}}(\mathbf{r}) - u_{\mathbf{r}'}(\mathbf{r})}{t}. \end{aligned}$$

THEOREM 3.2 *Suppose that u and v are generated by a monopole at $\mathbf{b} \in D$ and a dipole at $\mathbf{c} \in D$ with orientation ν . Then the inner product (u, v) depends on ν and the vector*

$$(3.14) \quad \mathbf{a} = \mathbf{b} - \mathbf{c} = (x_a, y_a).$$

More precisely, let $a = |\mathbf{a}|$ and let $\phi = \arctan(y_a/x_a)$ be the angle formed by the x -axis and \mathbf{a} . Then

$$(3.15) \quad (u, v) = -\frac{ik}{\pi} \int_{-\pi/2}^{\pi/2} e^{-ika \sin(\theta-\phi)} \sin(\theta - \nu) d\theta.$$

In particular, when $\mathbf{b} = \mathbf{c}$ and for arbitrary orientation ν ,

$$(3.16) \quad (u, v) = -\frac{ik}{\pi} \int_{-\pi/2}^{\pi/2} \sin(\theta - \nu) d\theta = \frac{2ik}{\pi} \sin(\nu).$$

PROOF: The proof exploits the definition of a dipole, the bilinearity of the inner product, and the inner product of two monopoles as derived above.

We define $\mathbf{c}_t = \mathbf{c} + t\mathbf{d}$, $\mathbf{a}_t = \mathbf{b} - \mathbf{c}_t$, $a_t = |\mathbf{a}_t|$, and ϕ_t to be the angle formed by the x -axis and \mathbf{a}_t . Referring to Figure 3.2, we observe

$$\begin{aligned} a_t &= a - t \cos(\nu - \phi), \\ \phi_t &= \phi - \arcsin \frac{t \sin(\nu - \phi)}{a_t}, \end{aligned}$$

from which

$$\begin{aligned} (3.17) \quad \lim_{t \rightarrow 0} \frac{a_t \sin(\theta - \phi_t) - a \sin(\theta - \phi)}{t} &= \left. \frac{d}{dt} a_t \sin(\theta - \phi_t) \right|_{t=0} \\ &= -\sin(\theta - \nu). \end{aligned}$$

Let v_t denote a monopole located at \mathbf{c}_t . Then

$$(3.18) \quad (u, v) = -\lim_{t \rightarrow 0} \frac{(u, v_t) - (u, v_0)}{t}.$$

Combining (3.2) and (3.17) with (3.18) yields the desired result (3.15). □

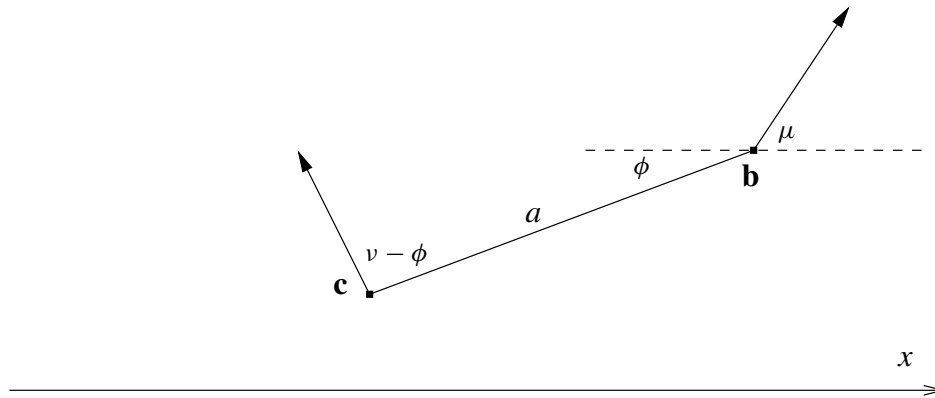


FIGURE 3.2. Two dipoles **b** and **c** with orientations μ and ν .

3.3 Inner Product for Two Dipoles

The computation of the inner product of two dipoles closely follows that of a monopole and dipole given above, yielding the following theorem:

THEOREM 3.3 *Suppose that u and v are generated by two dipoles at $\mathbf{b}, \mathbf{c} \in D$ with orientations μ and ν . Then the inner product (u, v) depends on the orientations and the vector*

$$(3.19) \quad \mathbf{a} = \mathbf{b} - \mathbf{c} = (x_a, y_a).$$

More precisely, let $a = |\mathbf{a}|$ and let $\phi = \arctan(y_a/x_a)$ be the angle formed by the x -axis and \mathbf{a} . Then

$$(3.20) \quad (u, v) = \frac{k^2}{\pi} \int_{-\pi/2}^{\pi/2} e^{-ika \sin(\theta-\phi)} \sin(\theta - \mu) \sin(\theta - \nu) d\theta,$$

where the unit vectors μ and ν are regarded as the angles they form with the x -axis; see Figure 3.2. In particular, when $\mathbf{b} = \mathbf{c} \in D$,

$$(3.21) \quad (u, v) = \frac{k^2}{\pi} \int_{-\pi/2}^{\pi/2} \sin(\theta - \mu) \sin(\theta - \nu) d\theta = \frac{k^2}{2} \cos(\mu - \nu).$$

3.4 Inner Product for Two Multipoles

We refer to the function $u(\mathbf{r}) = H_m(kr)e^{im\theta}$ as the wave generated by a multipole of order m centered at $\mathbf{r}' \in \mathbb{R}^2$, where $\mathbf{r} - \mathbf{r}'$ has polar coordinates (r, θ) ,

$$(3.22) \quad r = [(x - x')^2 + (y - y')^2]^{1/2}, \quad \theta = \arctan \frac{y - y'}{x - x'}.$$

The inner product of two multipoles centered at \mathbf{r}' has a very simple form.

THEOREM 3.4 *Suppose that u and v are generated by two multipoles of order m and n , respectively, centered at some point \mathbf{r}' above the x -axis. Then*

$$(3.23) \quad (u, v) = \begin{cases} 1, & m = n, \\ 2(-1)^{(1+|m-n|)/2}/(|m - n|\pi), & m - n \text{ odd,} \\ 0, & \text{otherwise.} \end{cases}$$

PROOF: The proof follows that of Theorem 3.1 except that the circular arc of radius r below the x -axis is centered at $\mathbf{r}' = (x', y')$. The multipoles are then given by

$$(3.24) \quad u(\mathbf{r}) = H_m(kr)e^{im\theta}, \quad v(\mathbf{r}) = H_n(kr)e^{in\theta},$$

their normal derivatives (see, e.g., [1, 9.1.27]) computed from

$$(3.25) \quad \frac{\partial H_m(kr)}{\partial r} = \frac{k}{2}(H_{m-1}(kr) - H_{m+1}(kr)),$$

and the asymptotic forms of the Hankel functions given by (3.10). Now we obtain

$$\begin{aligned} (u, v) &= \lim_{r \rightarrow \infty} \frac{i}{4} \int_{\pi + \arcsin(y'/r)}^{2\pi - \arcsin(y'/r)} \left[u(\mathbf{r}) \frac{\partial \bar{v}(\mathbf{r})}{\partial r} - \bar{v}(\mathbf{r}) \frac{\partial u(\mathbf{r})}{\partial r} \right] r d\theta \\ &= \lim_{r \rightarrow \infty} \frac{i}{4} \int_{\pi}^{2\pi} \left[u(\mathbf{r}) \frac{\partial \bar{v}(\mathbf{r})}{\partial r} - \bar{v}(\mathbf{r}) \frac{\partial u(\mathbf{r})}{\partial r} \right] r d\theta \\ &= \frac{1}{\pi} \int_{\pi}^{2\pi} e^{i(m-n)(\theta - \pi/2)} d\theta, \end{aligned}$$

from which the theorem is established. □

4 Other Unbounded Curves

The foregoing discussion has been limited to representation of the field of compact sources on a line. A review of the discussion reveals, however, that none of the argument is limited to a line: each fact applies equally to other curves that divide the plane into two unbounded regions, one of which contains the sources.

Let $C \subset \mathbb{R}^2$ be a curve with parametrization $\lambda : \mathbb{R} \rightarrow \mathbb{R}^2$, so that $\lambda(t) \in C$ for $t \in \mathbb{R}$. We suppose that C is simple (λ is a one-to-one map), that C is unbounded ($|\lambda(t)| \rightarrow \infty$ as $t \rightarrow \pm\infty$), and C carves out a sector of the plane,

$$(4.1) \quad \lim_{t \rightarrow -\infty} \frac{\lambda(t)}{|\lambda(t)|} = \mathbf{d}_-, \quad \lim_{t \rightarrow \infty} \frac{\lambda(t)}{|\lambda(t)|} = \mathbf{d}_+,$$

for some \mathbf{d}_- and \mathbf{d}_+ . Under these assumptions, C divides the plane into two regions. If u and v are waves whose sources lie entirely in the same region, the bilinear form

$$(4.2) \quad (u, v) = \frac{i}{4} \int_C [u\bar{v}_n - \bar{v}u_n] d|C|$$

is independent of C other than the unit vectors \mathbf{b} and \mathbf{c} . Furthermore, (u, u) is positive for $u \neq 0$ provided that the direction of the normal to C is chosen to point away from the source region, the integration is taken in the counterclockwise direction relative to the sources, and $\mathbf{b} \neq \mathbf{c}$. Hence, under these conditions, the bilinear form is an inner product. We remark that the plane could alternatively be divided into regions by a curve C satisfying (4.1) with $\mathbf{b} = \mathbf{c}$, giving an infinite enclosed strip. In this case, if the sources are in the strip, the bilinear form is an inner product, whereas if the sources are outside, $(u, u) = 0$ for all waves u .

The following theorem restates the results of the previous section for the inner products of point sources for a simple, unbounded curve of the type just presented. Its proof exactly follows that for the line and is omitted.

THEOREM 4.1 *Suppose that C is an unbounded curve dividing the plane into two regions and (u, v) is the inner product defined by (4.2), where u and v are point sources located at \mathbf{b} and \mathbf{c} lying in one of the regions. Suppose β and γ are the orientations of the unit vectors \mathbf{d}_- and \mathbf{d}_+ given in (4.1), where $\lambda(t)$ traverses C counterclockwise, for increasing t relative to \mathbf{b} and \mathbf{c} . Finally, suppose $\mathbf{a} = \mathbf{b} - \mathbf{c} = (x_a, y_a)$, $a = |\mathbf{a}|$, and $\phi = \arctan(y_a/x_a)$.*

(1) **INNER PRODUCT OF TWO MONOPOLES.** *If u and v are monopoles, then*

$$(4.3) \quad (u, v) = \frac{1}{\pi} \int_{\beta}^{\gamma} e^{-ika \cos(\theta-\phi)} d\theta.$$

(2) **INNER PRODUCT OF A MONOPOLE AND A DIPOLE.** *If u is a monopole and v is a dipole with orientation v , then*

$$(4.4) \quad (u, v) = \frac{k}{\pi} \int_{\beta}^{\gamma} e^{-ika \cos(\theta-\phi)} \cos(\theta - v) d\theta.$$

(3) **INNER PRODUCT OF TWO DIPOLES.** *If u and v are dipoles with orientations μ and v , respectively, then*

$$(4.5) \quad (u, v) = \frac{k^2}{\pi} \int_{\beta}^{\gamma} e^{-ika \cos(\theta-\phi)} \cos(\theta - v) \cos(\theta - \mu) d\theta.$$

(4) **INNER PRODUCT OF TWO MULTIPOLES.** *If $\mathbf{b} = \mathbf{c}$ and u and v are multipoles of order m and n , respectively, then*

$$(4.6) \quad (u, v) = \frac{1}{\pi} \int_{\beta}^{\gamma} e^{i(m-n)(\theta-\pi/2)} d\theta.$$

5 Analytical and Numerical Examples

In this section, we present examples illustrating how the inner product can be used to construct an orthonormal basis of \mathcal{W} .

As is well known, the SVD of the operator $A : L^2(D) \rightarrow \mathcal{W}$ can be obtained from the eigendecomposition of a truncated $N \times N$ Gram matrix of inner products $B = \{(u_m, u_n)\}$, where $u_n = Ae_n$ and $\{e_n : n \in \mathbb{Z}\}$ is an orthonormal basis

for $L^2(D)$. (This procedure “squares the system,” so is not advisable in some applications.) In particular, suppose $B = WDW^h$, where W is unitary and D is diagonal. If w_i and w_j are two columns of W , with $w_i = \langle w_{1i}, \dots, w_{Ni} \rangle^T$ and $w_j = \langle w_{1j}, \dots, w_{Nj} \rangle^T$, then we define wave functions $s_i = \sum_k w_{ki} u_k$ for $i = 1, \dots, n$, and obtain

$$\begin{aligned}
 (5.1) \quad (s_i, s_j) &= \sum_{k=1}^n \sum_{l=1}^n w_{ki} \bar{w}_{lj} (u_k, u_l) \\
 &= w_j^h B w_i \\
 &= \delta_{ij} d_i,
 \end{aligned}$$

where d_i is the i^{th} element on the diagonal of D . Thus $\{s_1, \dots, s_N\}$ is an orthogonal set in \mathcal{W} with $(s_i, s_i) = d_i$.

In the examples, we replace the map A from the source region (to the field region) by a map \tilde{A} from the boundary of the source region, which is sufficient and simplifies the analysis. In the domain we will have Dirichlet data (Examples 1 and 2) or a single-layer density (Examples 3 and 4), and, in a slight abuse of notation, we use \tilde{A} to denote the operator in each case.

Example 1. Suppose all sources are contained within a disk D of radius r_0 centered at $\mathbf{r}' = (0, y_0)$ with $y_0 > r_0$. Complex exponentials $\{e_n(\theta) = e^{in\theta} : n \in \mathbb{Z}\}$ form an orthonormal basis for $L^2(\partial D)$ under the usual inner product. The map $\tilde{A} : L^2(\partial D) \rightarrow \mathcal{W}$ is given by

$$(5.2) \quad u_n(x) = (\tilde{A}e_n)(x) = \frac{H_n(kr)}{H_n(kr_0)} e^{in\theta}, \quad n \in \mathbb{Z},$$

where $r = \sqrt{x^2 + y_0^2}$ and $\theta = \arctan(-y_0/x)$. From Theorem 3.4,

$$(u_m, u_n) = \frac{1}{H_m(kr_0)\bar{H}_n(kr_0)} \begin{cases} 1, & m = n, \\ 2(-1)^{(1+|m-n|)/2}/(|m-n|\pi), & m - n \text{ odd}, \\ 0, & \text{otherwise.} \end{cases}$$

For $r_0 = 1$, $y = \frac{3}{2}$, and $k = 10$, we truncate the matrix $B = \{(u_m, u_n)\}$ at $|n| \leq n_{\max} = 25$ ($N = 51$), for which all eigenvalues $d_1 > \dots > d_N$ agree with other truncations with $n_{\max} > 25$ to within $5 \cdot 10^{-15}$. Here $d_1 = 31.3$ and $d_{35} = 9.97 \cdot 10^{-15}$; the singular values $\sqrt{d_1}, \dots, \sqrt{d_{35}}$ are shown in Figure 5.2. The singular functions $v_i = s_i/\sqrt{d_i} \in \mathcal{W}$, $i = 1, \dots, 8$, are plotted in Figure 5.1.

The analogous computation was done for $k = 100$, for which $n_{\max} = 135$ suffices. Singular values $\sqrt{d_1}, \dots, \sqrt{d_{145}}$ are shown with those for $k = 10$ in Figure 5.2, and the singular functions v_1, \dots, v_8 are plotted in Figure 5.3.

Example 2. We suppose again that all sources are contained within a disk D of radius r_0 and ask about the singular functions on two horizontal lines, one above and

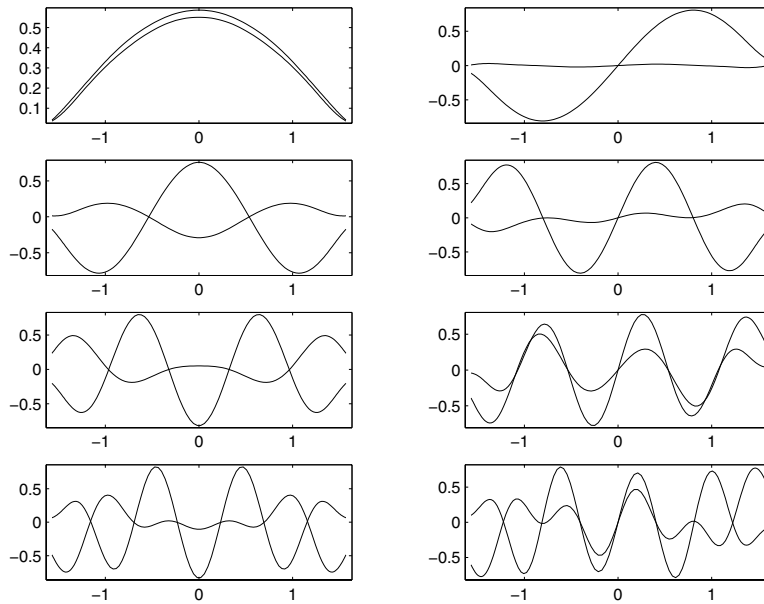


FIGURE 5.1. Singular functions v_1, \dots, v_8 from Example 1 for $k = 10$ are shown, each divided by monopole u_0 to normalize scale and oscillations. They are plotted along the entire x -axis as a function of $\theta \in [-\frac{\pi}{2}, \frac{\pi}{2}]$ with $x = y_0 \tan \theta$. Real and imaginary parts are shown.

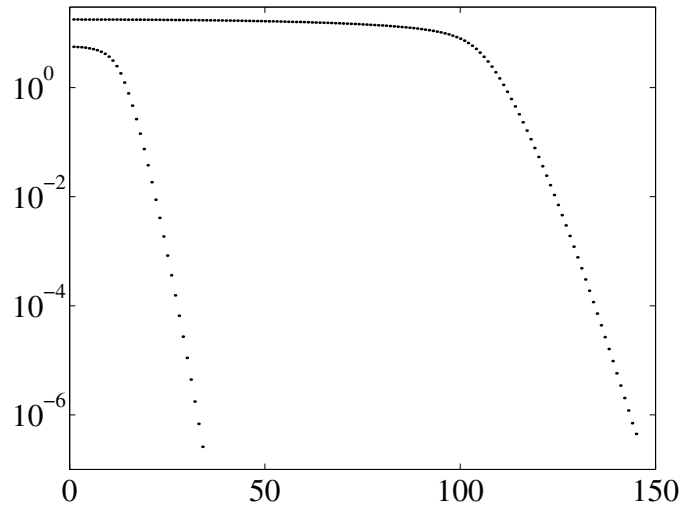


FIGURE 5.2. The singular values of the operator A in Example 1 are shown on a log scale, in decreasing order, for $k = 10$ (shorter sequence) and $k = 100$.

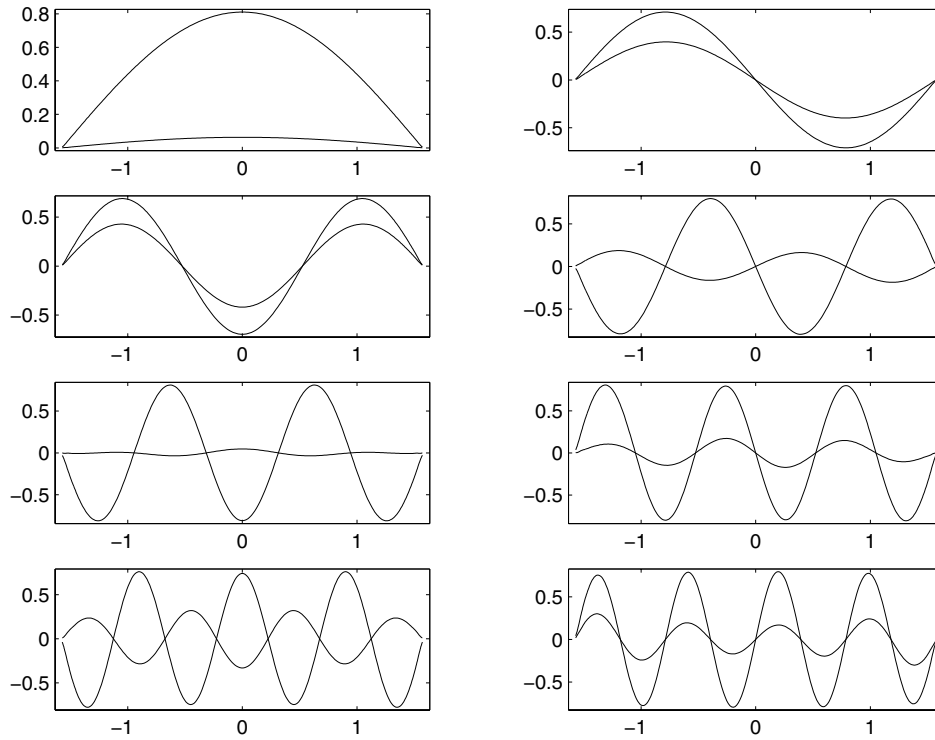


FIGURE 5.3. Singular functions as in Figure 5.1 but for $k = 100$.

one below D . This is the limiting case of an enclosing rectangle of fixed height and increasing width. Reasoning from Green’s second theorem (as in Theorem 2.1), we observe that two wave functions u and v from sources inside D have inner product (u, v) that is invariant through the limiting process; in fact, it can be computed most simply on the boundary ∂D . For multipole sources

$$(5.3) \quad u_n(\mathbf{r}) = H_n(k|\mathbf{r} - \mathbf{r}'|)e^{in\theta}, \quad n \in \mathbb{Z},$$

at the center \mathbf{r}' of D , we obtain

$$(5.4) \quad (u_m, u_n) = 2\delta_{mn}.$$

(On ∂D the integrand of the inner product is a constant times $e^{i(m-n)\theta}$, so $(u_m, u_n) = c_n\delta_{mn}$. Now employ Theorem 3.4 or, more directly, the Wronskian for H_n .) Thus the multipoles, scaled by $1/\sqrt{2}$, form an orthonormal basis on the two parallel lines.

Although the multipole u_n “radiates energy” that is invariant with n , its field values grow exponentially in n on ∂D for $|n| > kr_0$. The exponential growth typically makes multipoles an unsuitable basis for a source region very different from a disk.

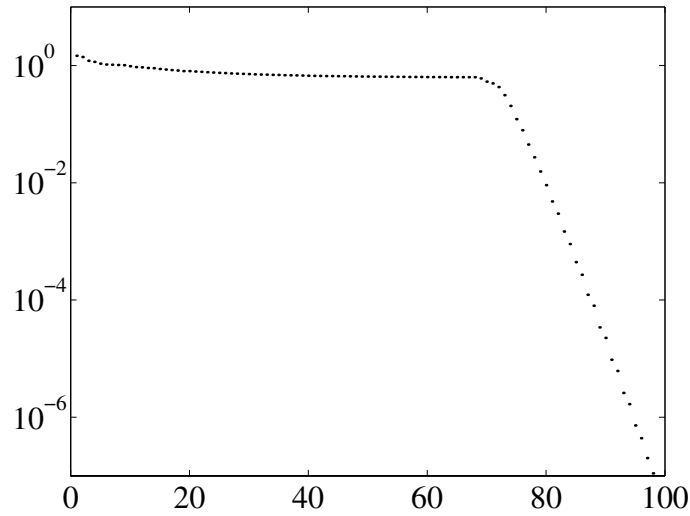


FIGURE 5.4. The singular values of the operator A in Example 3.

Example 3. Next we consider monopole sources on the boundary of the rectangle

$$(5.5) \quad M = \{(x, y) : |x| \leq a, |y - y_0| \leq b\}, \quad y_0 > b;$$

namely, we represent the waves on \mathbb{R} with a single-layer potential arising from a density η on the boundary ∂M . The density is discretized on each edge of the rectangle with Gauss-Legendre quadrature, yielding a set of monopoles as sources. As in Example 1, the eigendecomposition of the Gram matrix yields an orthonormal basis for \mathcal{W} .

For $a = 10, b = 1, y_0 = 4$, and $k = 10$, we choose 150 nodes on the horizontal edges and 20 nodes on the vertical edges, so $N = 340$. The integral (3.2) for the inner product of monopoles is discretized here with Gauss-Legendre quadrature containing 250 nodes. The singular values $\sqrt{d_1}, \dots, \sqrt{d_{98}}$ of the operator $\tilde{A} : L^2(\partial M) \rightarrow \mathcal{W}$ are plotted in Figure 5.4. Figure 5.5 shows the first two singular functions $v_1, v_2 \in \mathcal{W}$ and the integrands of the corresponding inner products (v_1, v_1) and (v_2, v_2) .

Example 4. In our final example, we examine the possibility of a source being focused to maximize or minimize the radiated energy that passes through a particular segment in the finite plane. We consider a double-layer density η on the segment M ,

$$(5.6) \quad M = \{(x, 4) : |x| \leq 10\}$$

as the source, and the segment

$$(5.7) \quad T = \{(x, 0) : |x| \leq 1\}$$

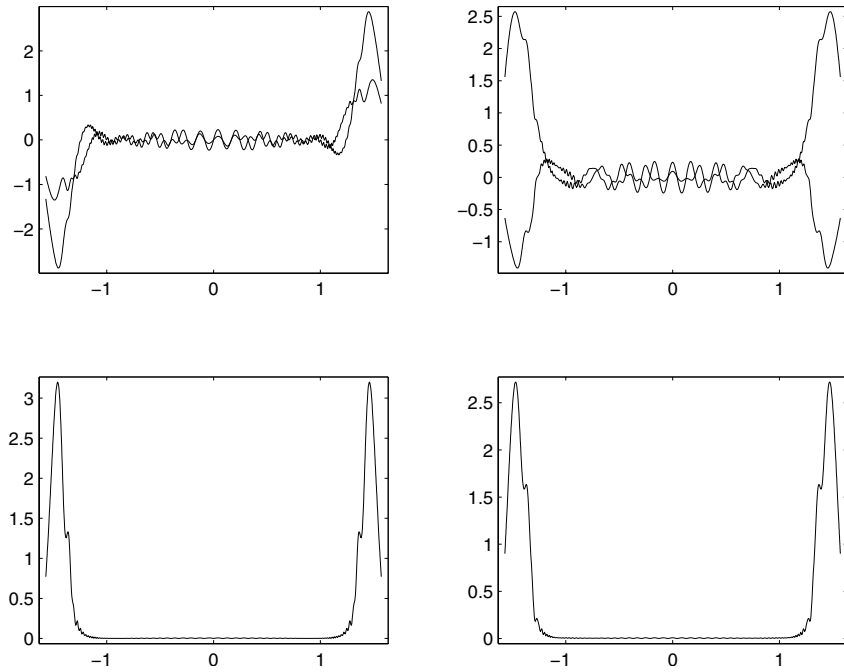


FIGURE 5.5. Top: Singular functions v_1 and v_2 divided by the potential of a monopole centered at $(0, y_0)$ from Example 3 are shown. As for Figure 5.1, they are plotted as functions of $\theta \in [-\frac{\pi}{2}, \frac{\pi}{2}]$ with $x = y_0 \tan \theta$. Bottom: Integrands of the corresponding inner products (v_i, v_i) multiplied by $\frac{dx}{d\theta}$.

on the x -axis as the target. The inner product presented above lacks positivity on finite curves, and in this setting is merely a bilinear form. No analytical formula for its value is available in this case; both M and T must be discretized. Again we choose $k = 10$, discretize the source region as for Example 3, and apply Gauss-Legendre quadrature (with 20 nodes) on the target segment. As in previous examples, we obtain the eigendecomposition of the Gram matrix $\{(u_m, u_n)\}$, where u_m is the wave on T due to a dipole on M .

For fixed 2-norm of the source density on M , Figure 5.6 shows the waveforms and the integrands of the bilinear form with the maximum and minimum radiation through the target segment in the direction $(0, -1)$.

6 Generalizations and Conclusions

We have described a method to represent the acoustic wave functions — the Helmholtz potentials — in an unbounded domain over which they oscillate an infinite number of cycles and decay too slowly to be sampled by standard methods with a finite number of points. Let u and v be two wave functions on \mathbb{R} arising

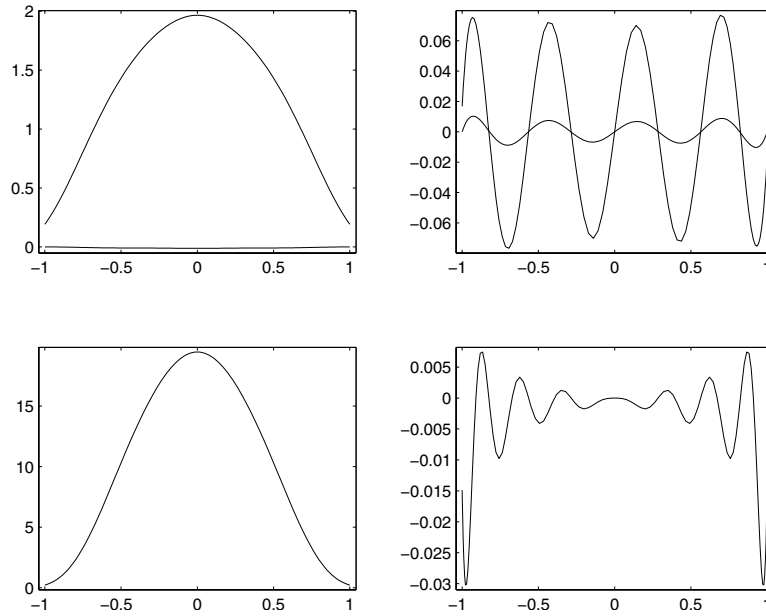


FIGURE 5.6. Top: Wave functions v_1 and v_2 on T having maximum positive and maximum negative flux through T . Bottom: The corresponding integrand of (v_i, v_i) in Example 4.

from two point sources in D (see Figure 2.1) separated by a distance a . It follows from the far-field asymptotics for the Hankel functions (3.10) that the main oscillation e^{ikr} of u and v vanishes in $u\bar{v}$ and $\frac{u}{v}$. A careful examination of them shows the following:

- (1) For a prescribed precision, it appears that the functions $u\bar{v}$ and $\frac{u}{v}$ oscillate only a finite number of cycles over \mathbb{R} , with the number of cycles of the main oscillation being about ka .
- (2) Similarly, the integrand of the inner product (u, v) oscillates about ka cycles.
- (3) For the domain D , separated from the x -axis and centered at (x_0, y_0) , the coordinate transformation $x : [-\frac{\pi}{2}, \frac{\pi}{2}] \rightarrow \mathbb{R}$,

$$(6.1) \quad x = x(\theta) = x_0 + y_0 \tan \theta,$$

reduces the integral (2.3) to

$$(6.2) \quad (u, v) = \frac{i}{4} \int_{-\pi/2}^{\pi/2} [u(x)\bar{v}_n(x) - \bar{v}(x)u_n(x)] \frac{dx}{d\theta} d\theta.$$

Let d be the diameter of D . The number of cycles of the main oscillation in the integrand of (6.2) is thus no more than kd , and the main oscillation is more or less evenly spread over $[-\frac{\pi}{2}, \frac{\pi}{2}]$ if the aspect ratio of D is close to 1.

(4) If the aspect ratio of D is large and if D is well separated from the x -axis, $y_0 > d$ (as in the case of Example 3 if the box M is vertically erected with $y_0 > a$), the transformation (6.1) is still reasonably efficient. Otherwise, as in the case of Example 3, other transformations perform better, for example,

$$(6.3) \quad \frac{dx}{d\theta} = \frac{2a + \pi b}{f(x)}$$

where

$$f(x) = f_1(x) + f_1(-x) \quad \text{and} \quad f_1(x) = \frac{(a+x)\sqrt{(a+x)^2 + y_0^2 - b^2} + by_0}{(a+x)^2 + y_0^2}$$

works well for Example 3.

Given a prescribed precision, the finite number of orthonormal basis functions we have constructed for the linear space \mathcal{W} give rise to a method to sample \mathcal{W} with a finite number of points.

OBSERVATION 6.1 *If the quadrature nodes $\{x_j\}$ are sufficient for the inner product (2.3) of \mathcal{W} , then they are also sufficient to sample \mathcal{W} . In other words, a wave function $u \in \mathcal{W}$ can be uniquely determined, up to the prescribed precision, at the points $\{x_j\}$, because u is uniquely determined by its Fourier coefficients $\{(u, u_i)\}$.*

The inner product (2.3) extends immediately to three dimensions; a paper reporting its analytical and computational tools is in preparation. A similar inner product also exists for the vector case, for example, of electromagnetic waves.

Bibliography

- [1] Abramowitz, M.; Stegun, I.; editors. *Handbook of mathematical functions*. Tenth printing. Applied Mathematics Series, 55. National Bureau of Standards, Washington, D.C., 1972.
- [2] Colton, D.; Kress, R. *Inverse acoustic and electromagnetic scattering theory*. 2nd ed. Applied Mathematical Sciences, 93. Springer, Berlin, 1998.

BRADLEY K. ALPERT
National Institute
of Standards and Technology
325 Broadway
Boulder, CO 80305-3328
E-mail: alpert@
boulder.nist.gov

YU CHEN
Courant Institute
251 Mercer St.
New York, NY 10012
E-mail: yuchen@cims.nyu.edu

Received April 2004.